This is the accept manuscript of the following article that appeared in final form in Applied Thermal Engineering 160: (2019) // 114054,
which has been published in final form at
https://doi.org/10.1016/j.applthermaleng.2019.114054.

Numerical model for liquid-to-liquid heat pumps implementing switching mode

Erik Salazar-Herran [a], Koldobika Martin-Escudero [a], Andrew G. Alleyne [b], Luis A. del Portillo-Valdes [a], Naiara Romero-Anton [a]

[a] ENEDI Research group, Department of Thermal Engineering, University of the Basque Country (UPV/EHU), Plaza Torres Quevedo 1, 48013 Bilbao, Spain

[b] Department of Mechanical Science and Engineering, University of Illinois at Urbana-Champaign, 1206 West Green Street, Urbana, IL 61801, USA

Email: erik.salazar@ehu.es

Tel.: + (34) 94 601 7322

ABSTRACT

Residential reversible liquid-to-liquid heat pump systems are effective systems to increase energy efficiency and decrease gas emissions of buildings that can supply both the cooling and heating demand of a building due to the reversible capability.

This document presents an innovative model developed in Matlab/Simulink that simulates the dynamic behavior of liquid-to-liquid heat pump systems. It is based on a physics-based numerical model capable to switch the refrigerant flow direction and the behavior of the PHEX (condenser or evaporator) according to the actual working mode. With this model, an analysis of the transient states during the switch of the operation mode is carried out.

The model was validated with experimental tests for both the heating and the cooling modes separately. For each working mode test, a sudden change in the working conditions of the system was forced to trigger a fast transient state. Then, the validated model was used to carry out a simulation of a switching mode, starting in the cooling mode and finishing in the heating mode.

Keywords: Reversible liquid-to-liquid heat pump; Dynamic modeling; Transient simulation; Finite control volume approach; Switching mode simulation

Nomenclature

Symbols

A_c	cross-sectional area [m^2]
A_s	heat transfer area [m^2]
COP	coefficient of performance [-]
c_p	specific heat [J/(kg·K)]
C_v	valve coefficient [m^2]
h	enthalpy [kJ/kg]
$\dot{h}$	enthalpy time derivative [kJ/(kg·s)]
L	distance between plates [m]
m	mass [kg]
$\dot{m}$	mass flow rate [kg/s]
N	number of finite volumes [-]
P	pressure [kPa]
$\dot{P}$	pressure time derivative [kPa/s]
$\dot{q}$	heat transfer rate [kW]

r	pressure ratio [-]
SC	subcooling [K]
SH	superheating [K]
t	time [s]
T	temperature [K]
V	volume [m^3]
$\dot{W}$	work rate [W]
x	space in the flow direction [m]

Greek letters

α	convection heat transfer coefficient [$kW/(m^2 \cdot K)$]
∂	partial derivative
ρ	density [kg/m^3]
η	efficiency [-]

Subscripts

comp	compressor
cond	condensation
cv	control volume
EEV	electronic expansion valve
evap	evaporation
h	at constant enthalpy
i	control volume index
in	inlet
ise	isentropic
out	outlet
P	at constant pressure
R	refrigerant
S	secondary fluid
vol	volumetric
W	wall/plate

1. Introduction

Reversible liquid-to-liquid heat pump systems (HP) are mechanical systems driven by electric energy with the objective of heating or cooling water by absorbing or transferring heat to the subsoil or a water reservoir. These systems are capable to switch the operation mode and work either heating the water or cooling it down in order to supply the heating or cooling demand. These systems are capable of producing hot and cold water throughout the year with low operating costs [1]. Moreover, compared with other heating and cooling systems such as air-source heat pump systems or electric water heaters, the performance of liquid-to-liquid HP is better, although the initial monetary investments are higher [2].

Dynamic analysis of systems provides information about the behavior and performance of systems under variations in external and operation conditions. These analyses can be carried out by means of different methodologies, such as experimental tests or computer simulations. The use of experimental tests is limited by the monetary costs, test times, external conditions and low versatility. On the contrary, computer simulations avoid many of these limitations, making it a widely used tool.

Many experimental studies for the dynamic analysis of heat pump systems have been carried out over the last few years, most of them for the monthly and annual energy performance assessment of the systems. Menegon et al. [3] developed a new dynamic test procedure for the characterization of an air-source heat pump system for cooling and heating working modes. Sebarchievici et al. [4] measured the performance parameters of a ground source heat pump (GSHP) during a month through experimental tests. Schibuola et al. [5] monitored a water source heat pump in Venice (Italy) for one year. Similarly, the energy performance of a GSHP system was evaluated by means of monitoring an office building for four years by Luo et al. [6].

Regarding dynamic computer simulations, depending on the purpose, they can be approached from two different points of view, macro- and micro-models. On the one hand, the purpose of simulations carried out by macro-models is to get a general view of the system behavior, over hours, days or months, in order to predict the seasonal performance of a given system. Usually, hourly dynamic variations of the external and operation conditions are taken into account to model the chosen system. The performance during transient states of operation conditions, such as start-up, shut-down and switching mode are not taken into account.

Dynamic macro-models of different heating, ventilation and air-conditioned (HVAC) systems have been studied over the last few years. Calise et al. [7] developed a dynamic model of three different layouts of solar heating and cooling systems and analyzed the daily transient energy performance. Specifically, dynamic macro-models of heat pump systems can be found in the recent bibliography. Buonomano et al. [8] analyzed the system's consumption, operation costs and environmental impact of a water loop heat pump system in hourly, daily and seasonal scales. The performance factor of a dual-source heat pump system was seasonally and annually analyzed by Grossi et al. [9]. Furthermore, the heat pump system included in a polygeneration system was dynamically simulated by Calise et al. [10]. The electric, thermal and economic analysis was presented on a daily, weekly and yearly basis.

On the other hand, dynamic micro-models can be used for dynamic computer simulations. This analysis focuses on the behavior of the system during short time periods in which transient states are given. Seconds-based time scales are usually used in order to understand the physical behavior of systems under fast transitory states.

In this line, the commercial software Thermosys [11] is able to carry out dynamic simulations of different vapor compression systems [12]. This software works in Matlab/Simulink and was developed from a physics-based model. For instance, non-reversible air source refrigeration

systems can be simulated with this software [13]. Similarly, Li et al [14], based on Thermosys software, developed a dynamic model of a cooling vapor compression cycle with which the shut-down and start-up operations were analyzed.

Regarding other programming environments, a transient modeling of a flash tank vapor injection heat pump system was developed by Qiao et al. [15, 16] using the Modelica environment to capture the transient heat transfer and flow phenomena. Similarly, Qiao et al. [17] presented a dynamic heat exchanger and frost growth model to account for the non-uniform frost formation during winter operation of a vapor injection heat pump system.

Concerning reverse-cycle dynamic modeling, Qiao et al. [18] presented a model in Modelica of an air-source heat pump system to analyze its transient characteristics during the defrosting cycle. The models used to simulate the behavior of the heat pump components were validated in [15, 17]. In addition, a physics-based model of the frost formation and melting is detailed and developed in [18]. Both frost formation and melting models, as well as the simulation during the defrosting cycle, were not compared with experimental tests.

The innovative model presented in this document is a micro-model that simulates the dynamic behavior of a reversible liquid-to-liquid HP system. As far as the authors know, there is no documentation in the bibliography where a dynamic micro-model is used to analyze the behavior of a liquid-to-liquid HP during short time transient states. Unlike the model used in [18], the presented model simulates the behavior of a residential liquid-to-liquid HP system instead of an air source heat pump by using the Finite Control Volume (FCV) approach instead of the Moving Boundary (MB) approach. Additionally, while in [18] the heat exchanger model always works in cross-flow, the presented model switches the heat exchanger connections between counter-flow and parallel-flow when a working mode switch is given.

This paper first presents the developed experimental tests and the equations used for the simulation model. Then, the validations of the model during heating and cooling operation modes are carried out separately. Finally, once the numerical model has been validated, the behavior of the system during the reverse period is analyzed.

This model is a useful design tool for heat pump system manufacturers. It can be used, for instance, to reduce the laboratory test times, to carry out parametric studies to optimize the system performance, or to check pre-development designs.

2. Methodology

2.1. Experimental tests description

The reversible liquid-to-liquid HP system was tested under dynamic laboratory conditions. The test bed is made up of the heat pump system and a climatic chamber. The test bed is supposed to emulate the actual working conditions of a ground/water source heat pump system for space heating and cooling with water.

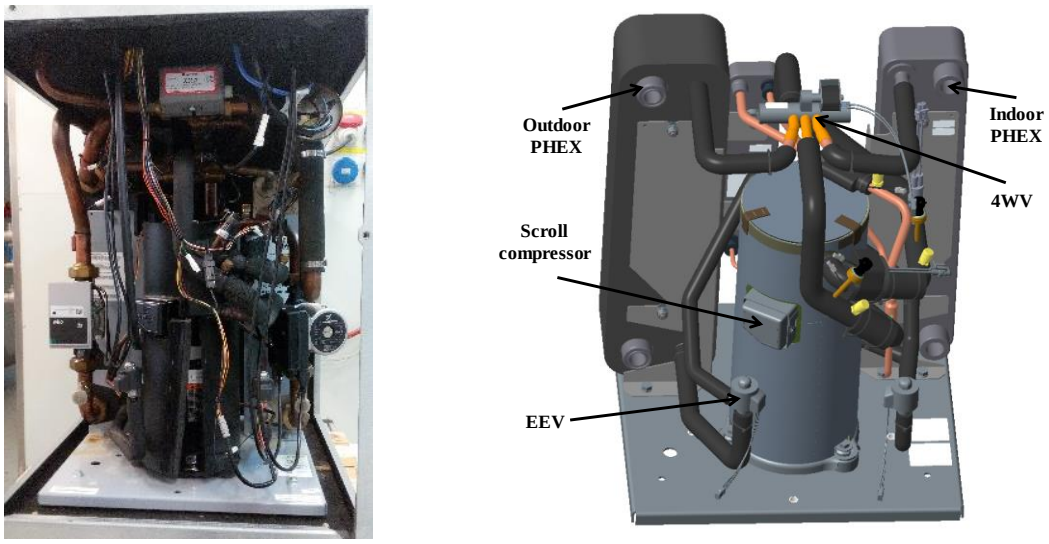

(a) (b)

Figure 1. Photography (a) and 3D image (b) of the heat pump system used.

The HP system is a commercial system of a nominal heating capacity of 5 kW that consists of one fixed speed and displacement compressor, one four-ways valve (4WV), one electronic expansion valve (EEV) and two refrigerant-to-liquid plate heat exchangers (PHEX). In Figure 1, a photograph and a 3D image of the heat pump system can be seen. Figure 2 shows the scheme of the HP. Some technical and geometrical specifications of the used scroll compressor and PHEX can be found in Table 1 and Table 2, respectively.

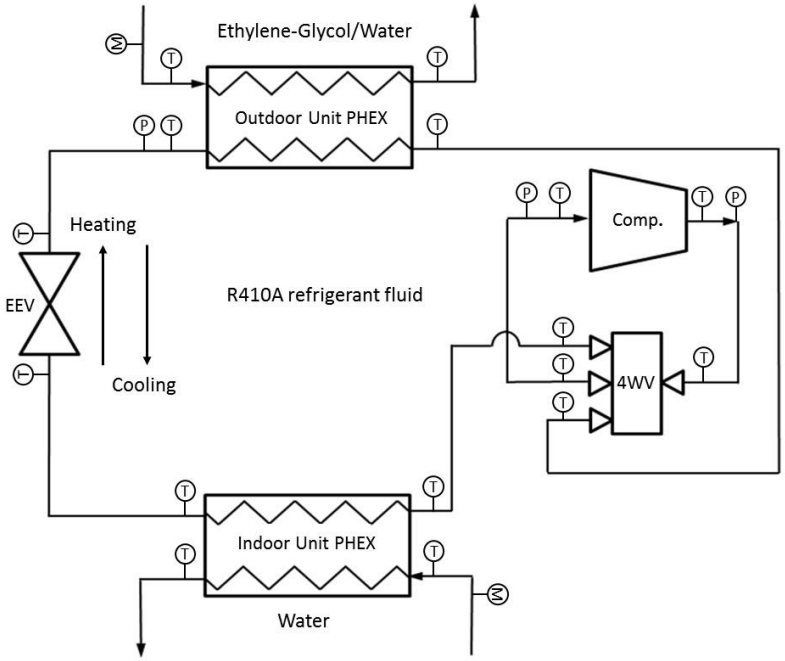

Figure 2. Tested heat pump system scheme.

Table 1. Specifications of the used scroll compressor.

Electric connection	220/240V 1~ 50Hz
Nominal heating capacity (kW)	5.0
Displacement (cm^3/rev)	19.34

$T_{evap} = -1℃ \quad SH = 4℃ \quad T_{cond} = 55℃ \quad SC = 3℃$

Heating power (kW)	6.20
Absorbed power (kW)	2.03
COP	3.06
Refrigerant mass flow rate (g/s)	23.60

Table 2. Specifications of the used PHEX.

	Indoor Unit	Outdoor Unit
Plates number	26	30
Dimensions (cm)	50 x 10 x 6.2	50 x 10 x 7.1
Primary fluid	R410A	R410A
Secondary fluid	Water	Ethylene-Glycol-Water
Total mass (kg)	6.35	7.01
Plates material	Stainless steel	Stainless steel

The PHEX of the heat pump system are connected to a climatic chamber that simulates the heat sources and sinks. One of them works as the indoor unit and the other as the outdoor unit of the HP. Due to the reversibility of the system, both can work as condenser and evaporator, depending on the current working mode. The refrigerant fluid used is R410A. In the indoor unit PHEX, the secondary fluid is water, which is connected to the climatic chamber simulating the thermal facilities of a house. In the outdoor unit PHEX, the secondary fluid is a mixture of 44% Ethylene-Glycol and 56% Water (brine).

When the working mode changes, the direction of the refrigerant also changes, while the direction of the secondary fluids remains the same. Because of this, the interaction between the refrigerant and the secondary fluid changes from counter-flow to parallel-flow or vice versa. It is widely known that a counter-flow PHEX connection has a better heat transfer performance than a parallel-flow connection [19, 20]. In this case, as the heat pump system used was optimized to work in the heating mode, both indoor and outdoor units are connected as counter-flow heat exchangers when the operation mode is heating. In cooling mode, both of them are connected in parallel-flow.

On the other hand, a mass flow distributor is located in the outdoor unit port that connects the PHEX and the EEV. As the refrigerant leaves the EEV as a two-phase fluid, the maldistribution of the fluid mass flow into the evaporator channels is very common [21]. This phenomenon can be minimized by placing a distributor in the inlet of the evaporator [22, 23]. As the system was optimized for working in the heating mode, the distributor is located in the entrance of the outdoor PHEX, which works as an evaporator during the heating mode. This distributor generates a pressure drop in the refrigerant fluid that was taken into account during the simulations.

Regarding the taken measurements, Table 3 presents the specifications of the devices used to measure the fluids temperatures, refrigerant pressures and secondary fluids mass flow rates. Figure 2 shows the measurements locations. Due to the accuracy of the measurement devices, secondary fluids temperatures and refrigerant pressures are the variables that will be used to validate the model.

Table 3. Specifications of the measuring equipment.

Measurement	Type	Uncertainty
Refrigerant temperature	NTC Thermistor Sensor	± 3 %
Refrigerant pressure	Pressure sensor 0 – 46~~00~~ bar	± 0.8 %
Secondary fluids temperature	Pt 100 resistance measurers	± 0.1 K

Secondary fluids mass flow	Flow meter 9 – 150 l/min	± 1 – 2 %

In order to validate the usefulness of the model to simulate fast transient states, such states were produced during the tests by forcing an abrupt change in the working conditions of the system (i.e. EEV current opening degree and water set-point temperature). The absolute average error and the normalized error (Eq. (1)) were used to validate numerically both heating and cooling modes. For this kind of simulation models, a normalized error smaller than 0.05 is usually acceptable [24].

$$Normalized\ error = \frac{\sum_{z=1}^{end}(simulation(z) - experimental(z))^2}{\sum_{j=1}^{end}(experimental(z))^2} \quad (1)$$

2.2. Heat Pump system modeling

A numerical model that simulates the dynamic behavior of a brine-to-water reversible heat pump has been developed. The model is made up of a scroll compressor, an electronic expansion valve and two PHEX. Both PHEX can operate as a condenser and evaporator. It has been developed in Matlab/Simulink.

The compressor and EEV are the components responsible for regulating the refrigerant mass flow, while the PHEX regulate the working pressures. The dynamics of the PHEXs are much slower than the dynamics of the compressor and the EEV [25, 26]. Thus, the compressor and EEV were modeled as static components. The 4WV was not modeled because, although in the actual system this valve allows the reversibility of the system, in the model it is not needed to reverse the cycle, as this is done with the numerical code by switching the component connections.

2.2.1. Compressor and EEV model

The compressor is statically modeled as a fixed speed and displacement unit. The equations utilized to simulate the refrigerant mass flow and the realized compression work are described in Park et al. [27]. The volumetric and the isentropic efficiencies of the compressor are calculated as a function of the pressure ratio ($r = P_{comp,out}/P_{comp,in}$). The curves of both efficiencies are fitted using the open design software of the compressor manufacturer.

The EEV static model calculates the refrigerant mass flow as a consequence of the current valve position. The EEV is assumed to have an isenthalpic thermodynamic behavior. The mass flow regulation is described by the relationship presented in Equation (2).

$$\dot{m}_{EEV} = C_v \cdot \sqrt{\Delta P \cdot \rho_{in}} \quad (2)$$

The curve that describe the valve coefficient with respect to the current number of steps for the used EEV was fitted using the commercial software 'IMST-ART' [28].

Table 4 presents the fitted equations and R^2 value for the compressor volumetric and isentropic efficiencies and for the EEV coefficient.

Table 4. Equations and R^2 value of compressor volumetric and isentropic efficiencies and EE coefficient curves.

	Equation	R^2
Volumetric efficiency [-]	$\eta_{vol} = 0.0058r^2 - 0.0997r + 1.1761$	0.926
Isentropic efficiency [-]	$\eta_{ise} = 0.0062r^2 - 0.0852r + 0.7942$	0.883

Valve coefficient [m^2]	$C_v = (0.133 \cdot steps + 1.011)E - 07$	0.990

2.2.2. Plate heat exchanger model

Unlike the compressor and EEV, plate heat exchangers are modeled dynamically, using partial differential equations for modeling both the refrigerant and secondary fluids and the intermediate plates.

At the time of modeling the behavior of the PHEX, pressure drops through the PHEX, maldistribution of the refrigerant at the inlet of the PHEX, the axial thermal conduction and the heat losses thorough the components and pipes insulation are neglected [24–26]. Fluid flow through PHEX is modeled as one-dimensional and finite control volume (FCV) approach is adopted to carry out the calculations.

Since the pressure drops are negligible and the secondary fluid mass flow rate is supposed to be constant during all the PHEX, the momentum conservation equation of both refrigerant and secondary fluids and the mass conservation equation of secondary fluids are not taken into account. Bearing all this in mind, four governing equations are needed to model the dynamic behavior of a PHEX.

The conservation of refrigerant energy, conservation of refrigerant mass, conservation of secondary fluid energy and conservation of intermediate plate energy are presented in Equations (3) - (6) respectively.

$$\frac{\partial(\rho_R A_c h_R)}{\partial t} - \frac{\partial(A_c P_R)}{\partial t} + \frac{\partial(\dot{m}_R h_R)}{\partial x} = 2\alpha_R L(T_R - T_W) \tag{3}$$

$$\frac{\partial(\rho_R A_c)}{\partial t} + \frac{\partial(\dot{m}_R)}{\partial x} = 0 \tag{4}$$

$$\frac{\partial(\rho_S A_c c_{p,S} T_S)}{\partial t} + \frac{\partial(\dot{m}_S c_{p,S} T_S)}{\partial x} = 2\alpha_S L(T_W - T_S) \tag{5}$$

$$\left(c_p m\right)_W \frac{\partial T_W}{\partial t} = \alpha_R A_s (T_R - T_W) + \alpha_S A_s (T_W - T_S) \tag{6}$$

Equations (3) - (6) are now transformed by applying the following steps:

- Equations are integrated over the length of the control volume, which in this case is the total length of the heat exchanger.
- The average values for the control volume of fluid and plate properties are taken, indicating them as $\rho_{R,i}, h_{R,i}, T_{R,i}, T_{S,i}, \rho_{S,i}, c_{p,S,i}, T_{W,i}, \alpha_{R,i}, \alpha_{S,i}$.
- It is assumed that the enthalpy and pressure are the independent variables in which depend on the other refrigerant fluid properties.

Once these steps are applied, the transformed equations of refrigerant energy, refrigerant mass, secondary fluid energy and plate energy are given in Equations (7) - (10).

$$V_{cv}\left[\left(\left|\frac{\partial\rho}{\partial P}\right|_h\right)_i h_{R,i} - 1\right]\dot{P}_R + V_{cv}\left[\left(\left|\frac{\partial\rho}{\partial h}\right|_P\right)_i h_{R,i} + \rho_{R,i}\right]\dot{h}_{R,i} + \dot{m}_{R,out}h_{R,out} - \dot{m}_{R,in}h_{R,in} = 2\alpha_{R,i}A_{s,cv}\left(T_{R,i} - T_{W,i}\right) \tag{7}$$

$$V_{cv}\left(\left|\frac{\partial\rho}{\partial P}\right|_h\right)_i \dot{P}_R + V_{cv}\left(\left|\frac{\partial\rho}{\partial h}\right|_P\right)_i \dot{h}_{R,i} + \dot{m}_{R,out} - \dot{m}_{R,in} = 0 \quad (8)$$

$$V_{cv}\rho_{S,i}c_{p,S,i}\dot{T}_{S,i} + \dot{m}_{S,i}c_{p,S,i}\left(T_{S,out} - T_{S,in}\right) = 2\alpha_{S,i}A_{s,cv}\left(T_{W,i} - T_{S,i}\right) \quad (9)$$

$$\left(c_p m\right)_{W,cv}\dot{T}_{W,i} = \alpha_{R,i}A_{s,cv}\left(T_{R,i} - T_{W,i}\right) + \alpha_{S,i}A_{s,cv}(T_{W,i} - T_{S,i}) \quad (10)$$

Now, this formulation can be extended to an N arbitrary number of finite and equal control volumes, taking into account the considerations followed in [24]. Note that Herschel et al. [24] modeled an air-to-refrigerant HEX and, in this case, the model is for a liquid-to-refrigerant HEX. This yields N more states that must be considered and integrated.

Taking into account the fact that the inlet and outlet refrigerant mass flow rates are known, 4N continuous states must be solved. Nevertheless, only 2N states must be solved together, as the secondary fluid energy equation and the plate energy equation can be solved separately, once heat transfer rates between fluids and plate are calculated. For this study, both PHEX were divided into twenty finite control volumes.

The convection heat transfer coefficients (HTC) were calculated by using the empirical correlations presented in Han et al. [29, 30]. On the other hand, both PHEX can work in parallel-flow and counter-flow connections, depending on the current operation mode. At the time of calculating heat transfer rates and secondary fluid temperature variation, the PHEX connections must be taken into account.

2.3. Operating procedure for switching mode

The model was used to simulate a switching mode, where the system starts working in the cooling mode and, in a given time, it changes to the heating mode. In the real systems, when switch the operation mode, the compressor is firstly stopped and the EEV is fully opened in order the pressures can be equalized. Once all the system is at the same pressure level, the order to switch the ports connection is given to the 4WV. Then, the compressor starts working again and the opening degree is regulated by the system control.

For the simulation, the inlet conditions and the time in which the mode want to be switched is previously fixed. The process followed in the simulation to switch the mode is automated in the numerical code and it is equal to the actual systems. The only difference is that the connections between components are switched without needing the 4WV.

Input conditions to the system will remain constant throughout the switching mode simulation. The inlet water temperature at 20 ºC, inlet brine temperature at 12 ºC and the mass flow rate of both water and brine at 0.25 kg/s. Regarding the EEV, it starts working at 72% of the opening grade. When the compressor is switched off, the EEV is fully opened in order to ease the equalization of the pressures. Once the system starts working again, it returns to the previous 72% of the opening grade. The compressor is estimated to take 3 seconds to totally stop. This stop time interval is due to the inertia of the compressor and depends mostly on compressor size.

3. Results and discussion

In this section, numerical results are presented. Since there are no test data available to validate the model during the reverse period, due to the difficulties to reproduce a real switch of the operation mode in the laboratory facilities, the heating and cooling modes have first been validated separately. Then, the switching mode results are presented and analyzed.

3.1. Heating mode validation

During the heating mode, the water setpoint temperature is initially placed at 30 ºC and is changed to 25 ºC. The brine setpoint temperature remains constant at -9 ºC. Figure 3 shows the comparison between test data and simulation results of both pressures and secondary fluids temperatures.

The normalized error between simulation results and experimental data for the pressures in the outdoor and indoor units are 1.8e-05 and 2.6e-05, respectively. Regarding water outlet temperature is 1.5e-04, while for the brine outlet temperatures it is 2.6e-04.

The absolute average errors are 1.94 kPa for the outdoor unit pressure, 8.11 kPa for the indoor unit pressure, 0.32 ºC for the water outlet temperature and 0.11 ºC for the brine outlet temperature.

It can be said that the model results fit accurately the experimental data.

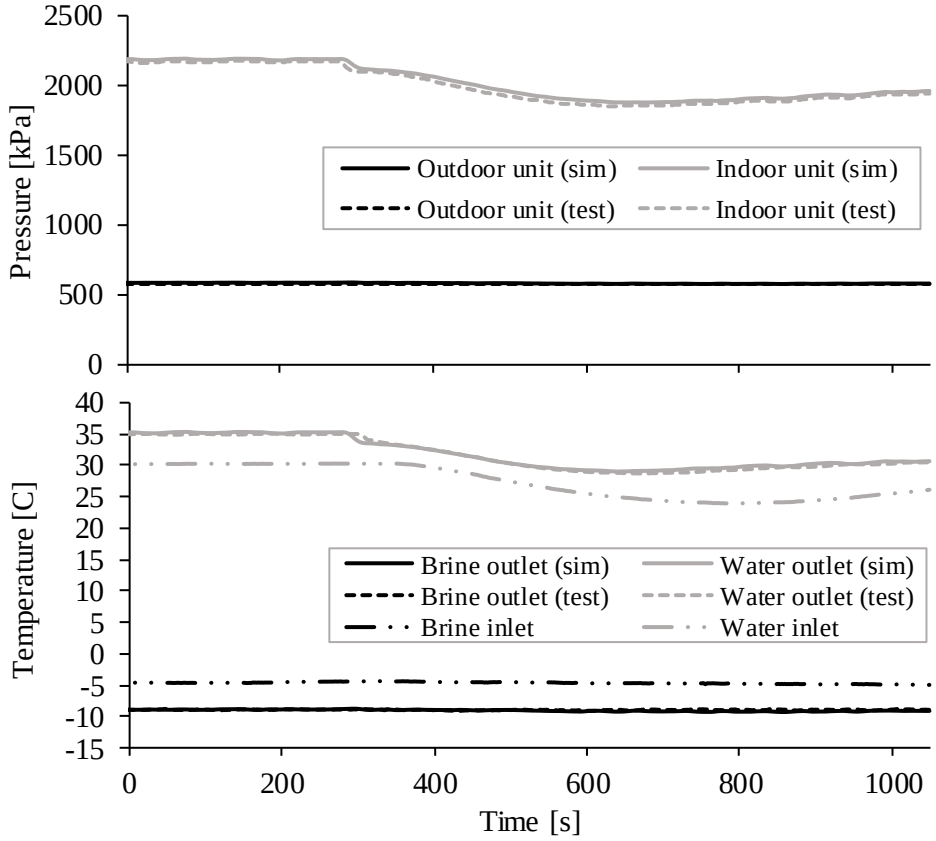

Figure 3. Test data and simulation results of the refrigerant pressures and temperatures during heating mode.

3.2. Cooling mode validation

During the cooling mode, the step is given in the outdoor unit. The brine set-point temperature starts at 30 ºC and finishes at 35 ºC. The water setpoint temperature remains constant at 13.5 ºC. The comparison between test data and simulations results for refrigerant working pressures and secondary fluid temperatures are presented in Figure 4.

The normalized error between simulation results and experimental data for the pressures in the outdoor and indoor units are 5.1e-04 and 9.3e-05, respectively. Regarding water outlet temperature is 1.3e-03, while for the brine outlet temperatures it is 3.7e-04.

The absolute average errors are 55.97 kPa for the outdoor unit pressure, 7.86 kPa for the indoor unit pressure, 0.22 ºC for the water outlet temperature and 0.75 ºC for the brine outlet temperature.

It can be asserted that the model accurately simulates the behavior of a liquid-to-liquid HP during cooling mode.

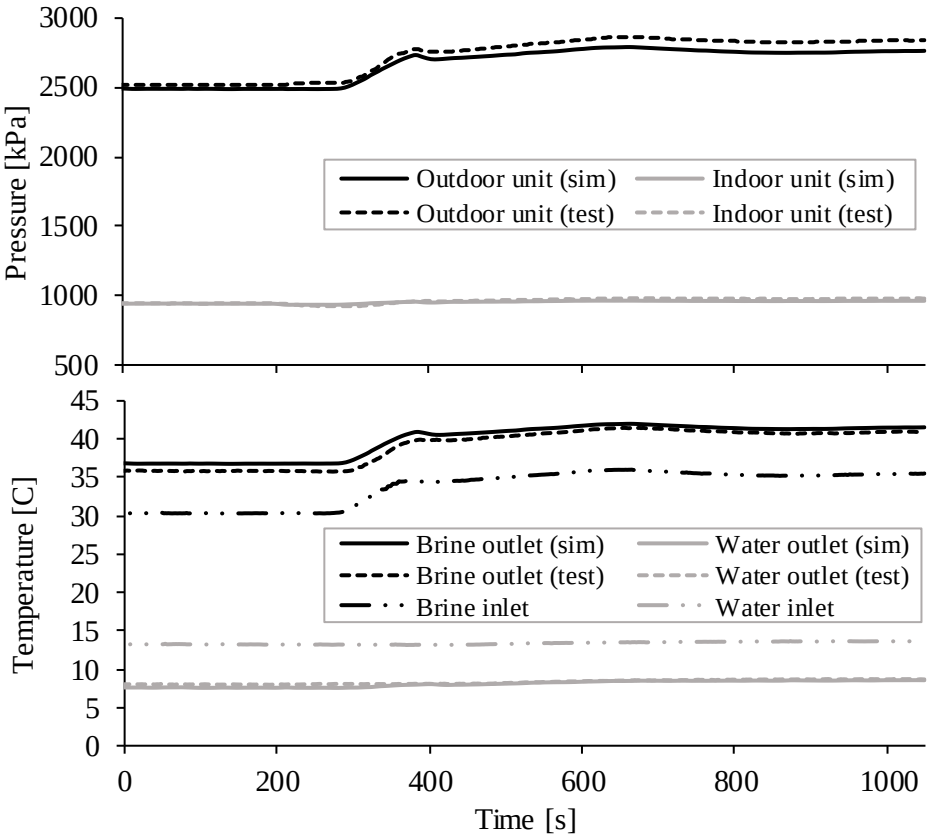

Figure 4. Test data and simulation results of the refrigerant pressures and temperatures during cooling mode.

3.3. Switching mode

Once the numerical model had been validated in both heating and cooling modes, a simulation of a switching mode was carried out. In all the figures of this section, the time in which the compressor is stopped and started-up has been marked.

The simulated mass flow rate of refrigerant is presented in Figure 5. The mass flow rates calculated in the compressor and the EEV are differentiated. As can be seen, the compressor mass flow rate goes to zero in three seconds, faster than the EEV ones, which depend on the slow dynamics of the heat exchangers, reaching zero at the moment when the pressures have been equalized. After the mode is switched, the compressors start working again, reaching a high value in a few seconds, then oscillates until an equilibrium with the mass flow rate calculated in the EEV is reached.

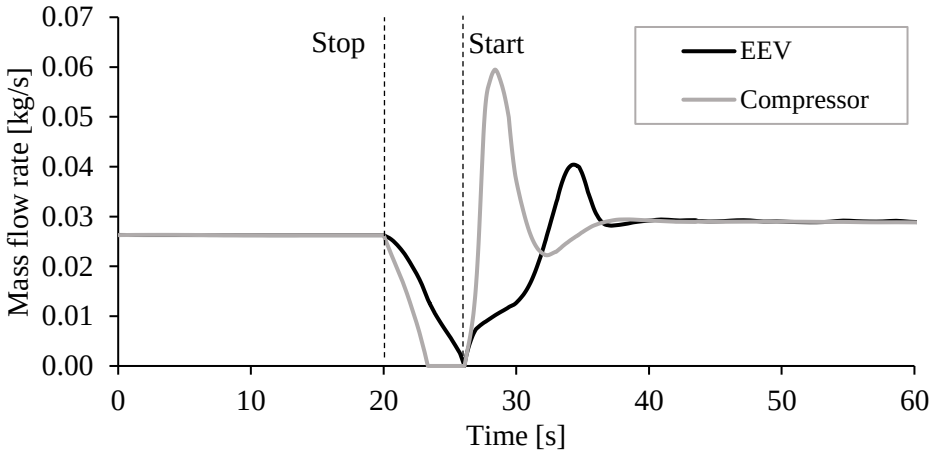

Figure 5. Refrigerant mass flow rate during reversible simulation.

Refrigerant fluid pressures can be seen in Figure 6. Initially, the outdoor unit PHEX works as a condenser (high pressure), while the indoor unit works as an evaporator (low pressure). After the switch, the opposite is true. Figure 6 clearly shows both the change in the working mode of the PHEX and the time at which pressures are equalized.

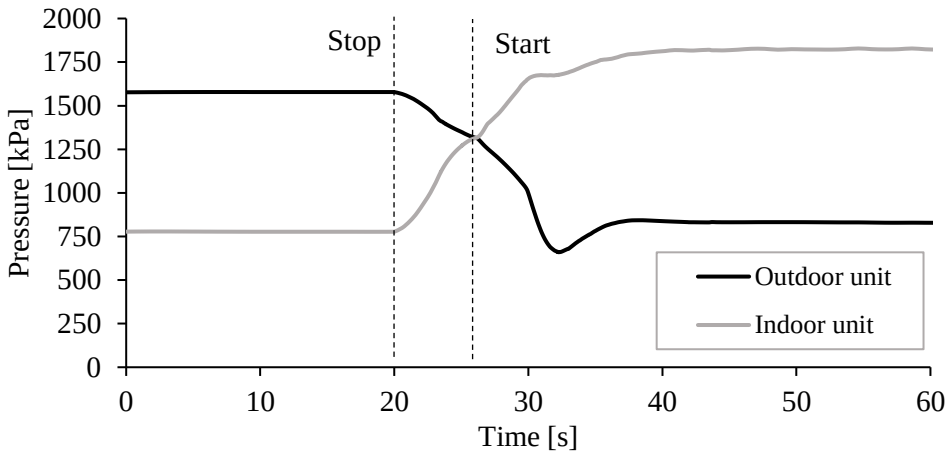

Figure 6. Refrigerant pressures during reversible simulation.

Figure 7 shows the refrigerant and brine temperatures in the outdoor PHEX inlet and outlet ports. During the cooling mode, port 1 and port 2 are the inlet and the outlet of the refrigerant side, respectively. During the heating mode, the port 2 is the inlet and the port 1 is the outlet. Brine is heated during the cooling mode and cooled down during the heating mode. When the compressor stops working, the temperatures of the refrigerant decrease because the refrigerant mass flow rate is almost null but the brine keeps flowing and cooling the refrigerant.

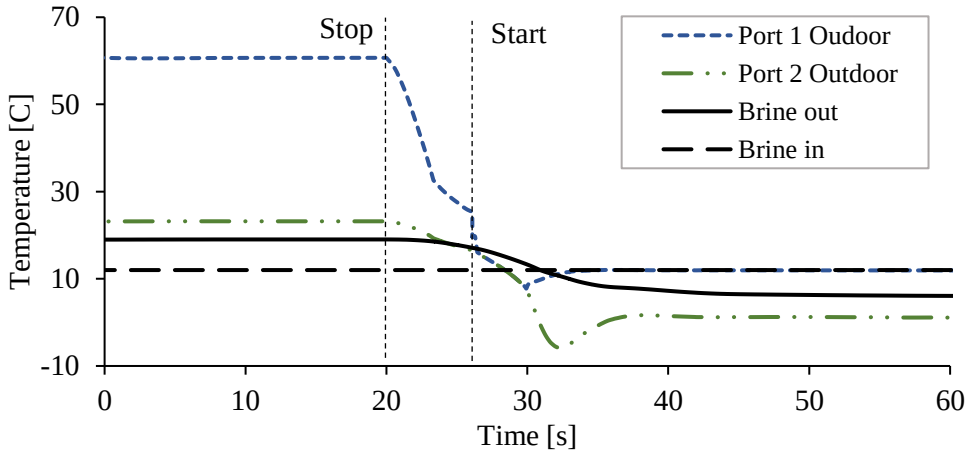

Figure 7. Outdoor PHEX inlet and outlet temperatures.

Figure 8 shows the refrigerant zones lengths inside the outdoor PHEX along the simulation. During cooling mode, in which the outdoor unit works as a condenser, it can be seen that the refrigerant is divided into three zones, superheated vapor, two-phase fluid and sub-cooled liquid. After the compressor shuts down, the sub-cooled zone disappears and the superheated zone continues decreasing until it disappears. As seen in Figure 7, for some time, both refrigerant temperatures are equal. This is because all the fluid inside the PHEX is a two-phase fluid, as can be seen in Figure 8. Then, as the refrigerant mass flow rate flows constantly again, the temperatures of the refrigerant start to separate one from the other and the superheated zone increases. The outdoor unit is now working as a two-zone evaporator.

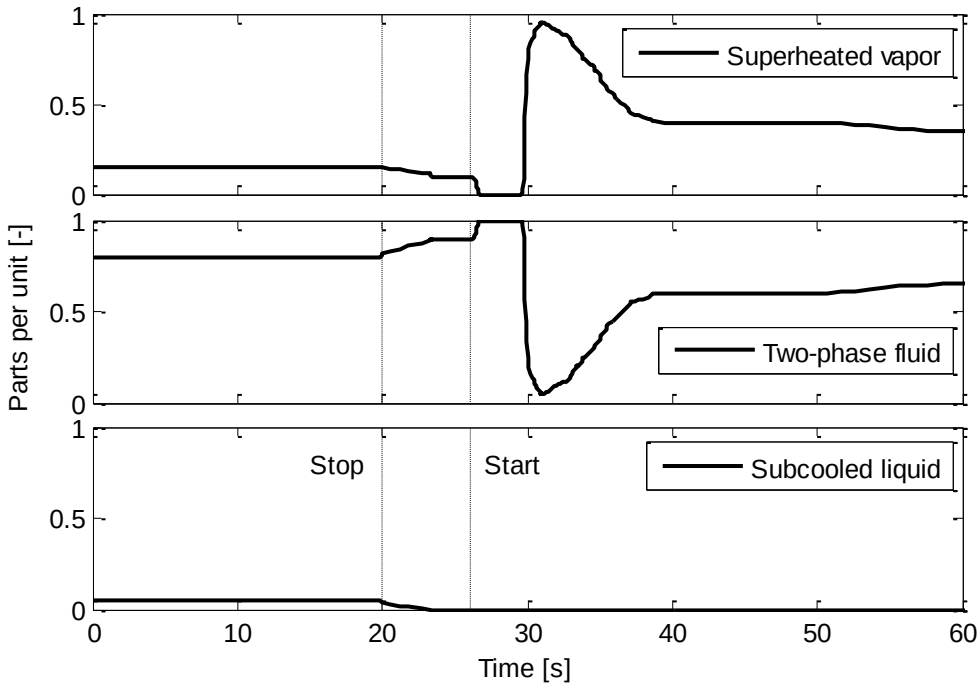

Figure 8. Outdoor PHEX vapor-liquid zones length per unit during reversible simulation.

Figure 9 shows the refrigerant and water temperatures in the indoor PHEX inlet and outlet ports. The port 2 is the inlet during the cooling mode and the outlet during the heating mode. Water is initially cooled down because it is working as an evaporator and, after the switch, it is heated as the PHEX works as a condenser. Refrigerant temperatures increase when the compressor is stopped as the water, which has a higher temperature than the refrigerant, continues to circulate and heat the refrigerant. Nevertheless, as the pressure also increases with time, although the

temperature increases, the two-phase zone of the refrigerant also increases. This can be seen in Figure 10. During the heating mode steady-state, the indoor PHEX works as a three-zones condenser.

It can be seen in Figure 7 and Figure 9 that both PHEX work in parallel-flow during cooling mode and in counter-flow during heating mode.

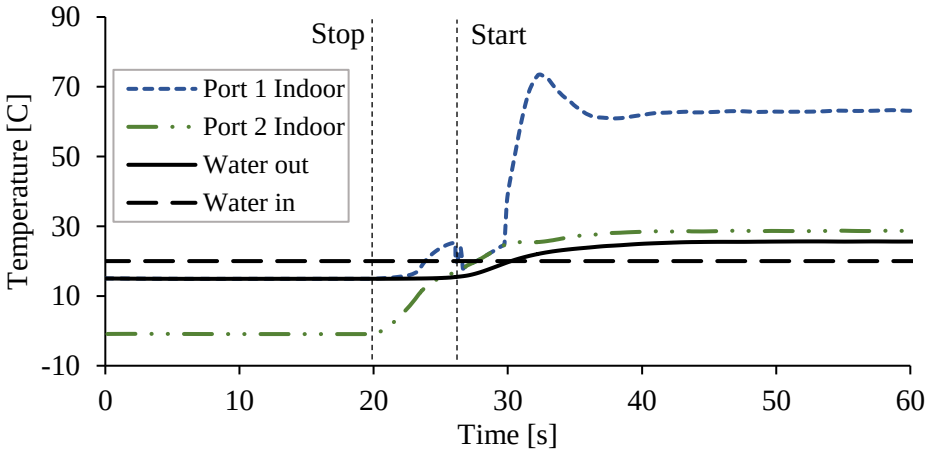

Figure 9. Indoor PHEX inlet and outlet temperatures.

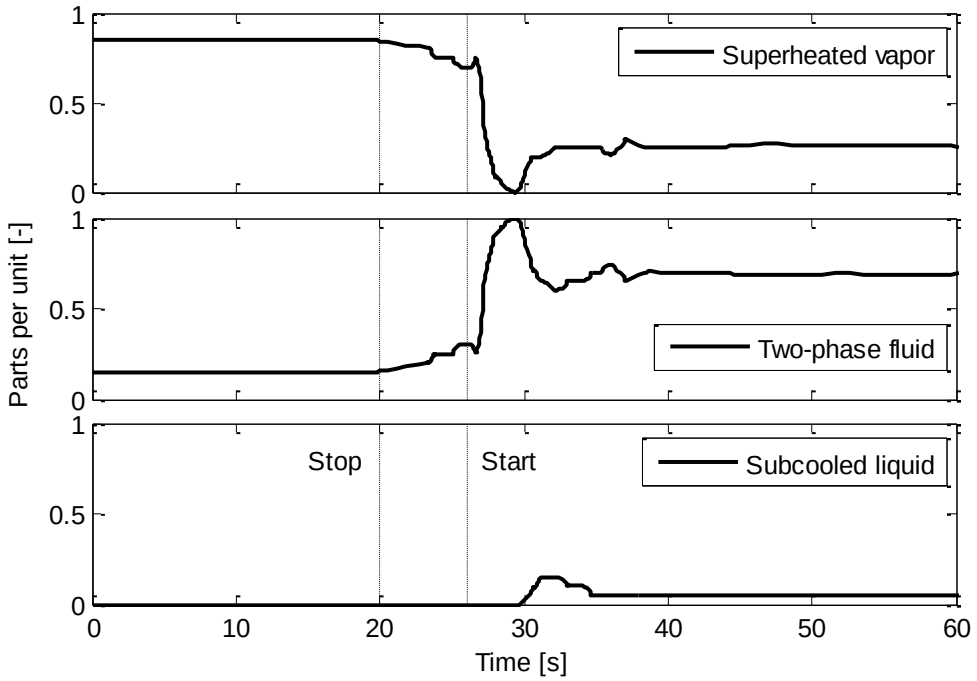

Figure 10. Indoor PHEX vapor-liquid zones length per unit during reversible simulation.

4. Conclusions

An analysis of the transient state during the switching mode of a reversible liquid-to-liquid heat pump system through a physics-based dynamic model is presented. The numerical mode has been validated for both the heating and the cooling working modes. The results show that the simulations fit accurately the experimental data, maintaining the normalized error below the accepted value for this kind of models.

The switching mode simulation shows that when the system stops working to carry out the switch, the refrigerant temperatures increase in the indoor unit and decrease in the outdoor unit, as the refrigerant mass flow rate is almost null, but the secondary fluid mass flow remains constant. Moreover, the entire refrigerant in both PHEX tends to be a two-phase fluid while the switch is giving until the refrigerant mass flow rate starts to flow again. The results also show that, from the time the command to switch the mode is given, the system needs around twenty seconds to reach the stationary state again, taking around seven seconds for equalize the pressures before switching the working mode.

REFERENCES

[1] IBRAHIM, Oussama, Farouk FARDOUN a Hasna LOUAHLIA-GUALOUS. Air source heat pump water heater : Dynamic modeling , optimal energy management and mini-tubes condensers [online]. 2014, 64, 1102–1116.

[2] SALAZAR-HERRAN, Erik, Koldobika MARTIN-ESCUDERO, Luis A. DEL PORTILLO-VALDES, Ivan FLORES-ABASCAL a Ana PICALLO-PEREZ. Residential Heat Pumps as Renewable Energy. In: *8th European Conference on Energy Efficiency and Sustainability in Architecture and Planning*. 2017, s. 163–170.

[3] MENEGON, Diego, Anton SOPPELSA a Roberto FEDRIZZI. Development of a new dynamic test procedure for the laboratory characterization of a whole heating and cooling system. *Applied Energy* [online]. 2017, 205, 976–990.

[4] SEBARCHIEVICI, Calin a Ioan SARBU. Performance of an experimental ground-coupled heat pump system for heating, cooling and domestic hot-water operation. *Renewable Energy* [online]. 2015, 76, 148–159.

[5] SCHIBUOLA, Luigi a Massimiliano SCARPA. Experimental analysis of the performances of a surface water source heat pump. *Energy and Buildings* [online]. 2016, 113, 182–188.

[6] LUO, Jin, Joachim ROHN, Manfred BAYER, Anna PRIESS, Lucas WILKMANN a Wei XIANG. Heating and cooling performance analysis of a ground source heat pump system in Southern Germany. *Geothermics* [online]. 2015, 53, 57–66.

[7] CALISE, F., M. DENTICE D'ACCADIA a A. PALOMBO. Transient analysis and energy optimization of solar heating and cooling systems in various configurations. *Solar Energy* [online]. 2010, 84(3), 432–449.

[8] BUONOMANO, Annamaria, Francesco CALISE a Adolfo PALOMBO. Buildings dynamic simulation: Water loop heat pump systems analysis for European climates. *Applied Energy* [online]. 2012, 91(1), 222–234.

[9] GROSSI, Ilaria, Matteo DONGELLINI, Agostino PIAZZI a Gian Luca MORINI. Dynamic modelling and energy performance analysis of an innovative dual-source heat pump system. *Applied Thermal Engineering* [online]. 2018, 142, 745–759.

[10] CALISE, Francesco, Rafal Damian FIGAJ a Laura VANOLI. A novel polygeneration system integrating photovoltaic/thermal collectors, solar assisted heat pump, adsorption chiller and electrical energy storage: Dynamic and energy-economic analysis. *Energy Conversion and Management* [online]. 2017, 149, 798–814.

[11] ALLEYNE, Andrew, Bryan RASMUSSEN a Joel JEDDELOH. *Thermosys Toolbox* [online]

[12] ALLEYNE, Andrew, Bryan RASMUSSEN, Michael KEIR a Brian ELDREDGE. Advances in Energy Systems Modeling and Control. In: *2007 American Control Conference* [online]. B.m.: IEEE, 2007, s. 4363–4373. ISBN 1-4244-0988-8.

[13] FASL, Joseph M. Modeling and Control of Hybrid Vapor Compression Cycles. 2013.

[14] LI, Bin a Andrew G. ALLEYNE. A dynamic model of a vapor compression cycle with shut-down and start-up operations. *International Journal of Refrigeration* [online]. 2010, 33(3), 538–552.

[15] QIAO, Hongtao, Vikrant AUTE a Reinhard RADERMACHER. Transient modeling of a flash tank vapor injection heat pump system – Part I: Model development. *International Journal of Refrigeration* [online]. 2015, 49, 169–182.

[16] QIAO, Hongtao, Xing XU, Vikrant AUTE a Reinhard RADERMACHER. Transient modeling of a flash tank vapor injection heat pump system – Part II: Simulation results and experimental validation. *International Journal of Refrigeration* [online]. 2015, 49, 183–194.

[17] QIAO, Hongtao, Vikrant AUTE a Reinhard RADERMACHER. Dynamic modeling and characteristic analysis of a two-stage vapor injection heat pump system under frosting conditions. *International Journal of Refrigeration* [online]. 2017, 84, 181–197.

[18] QIAO, Hongtao, Vikrant AUTE a Reinhard RADERMACHER. Modeling of transient characteristics of an air source heat pump with vapor injection during reverse-cycle defrosting. *International Journal of Refrigeration* [online]. 2018, 88, 24–34.

[19] LIU, Tsung-Lin, Ben-Ran FU a Chin PAN. Boiling two-phase flow and efficiency of co- and counter-current microchannel heat exchangers with gas heating. *International Journal of Heat and Mass Transfer* [online]. 2012, 55(21–22), 6130–6141.

[20] ÇENGEL, Yunus A. a Afshin J. GHAJAR. *Heat and mass transfer*. B.m.: McGraw Hill, 2004. ISBN 978-607-15-0540-8.

[21] PRABHAKARA RAO, B., P. KRISHNA KUMAR a Sarit K. DAS. Effect of flow distribution to the channels on the thermal performance of a plate heat exchanger. *Chemical Engineering and Processing: Process Intensification* [online]. 2002, 41(1), 49–58.

[22] ZHANG, Zhe, Sunil MEHENDALE, JinJin TIAN a YanZhong LI. Experimental investigation of distributor configuration on flow maldistribution in plate-fin heat exchangers. *Applied Thermal Engineering* [online]. 2015, 85, 111–123.

[23] YUAN, P., G.B. JIANG, Y.L. HE a W.Q. TAO. Performance simulation of a two-phase flow distributor for plate-fin heat exchanger. *Applied Thermal Engineering* [online]. 2016, 99, 1236–1245.

[24] PANGBORN, Herschel, Andrew G ALLEYNE a Ning WU. A comparison between finite volume and switched moving boundary approaches for dynamic vapor compression system modeling. *International Journal of Refrigeration* [online]. 2015, 53, 101–114.

[25] SHAH, R, Andrew G. ALLEYNE, Clark W BULLARD, B P RASMUSSEN a Predrag S Pega HRNJAK. Dynamic modeling and control of single and multi-evaporator subcritical vapor compression systems. *Industrial Engineering* [online]. 2003, 61801(217), 207.

[26] RASMUSSEN, BRYAN P; ALLEYNE, Andrew. *Dynamic modeling and advanced control of air conditioning and refrigeration systems*. B.m., 2005. University os Illinois at Urbana-Champaign.

[27] PARK, N., J. SHIN a B. CHUNG. A new dynamic heat pump simulation model with variable speed compressors under frosting conditions. *8th International Conference on Compressors and their Systems* [online]. 2013, 681–696.

[28] THERMAL AREA, Instituto de Ingeniería Enegética. *IMST-ART* [online]

[29] HAN, D.H., K.J. LEE a Y.H. KIM. Experiments on the characteristics of evaporation of R410A in brazed plate heat exchangers with different geometric configuration. *Applied Thermal Engineering* [online]. 2003, 23, 1209–1225.

[30] HAN, D.H., K.J. LEE a Y.H. KIM. The characteristics of brazed plate heat exchangers with different chevron angles. *Journal of the Korean Physical Society* [online]. 2003, 43, 66–73.